proach. Using these distributions and a model of the Jupiter ionosphere, we can conservatively conclude that the energy input into the Jovian aurora (*13*) by the measured electrons in the loss cone at a latitude (λ) of $\sim 20°$ is ~ 1.0 erg cm^{-2} s^{-1} and the ion input is about a factor of 10 less (*14*). Furthermore, the discovery of the ion and electron particle beams throughout the high-latitude magnetosphere suggests that at least a portion of these particles (whose loss cones at the locations where they are measured are only a small fraction of a degree) can also be lost into the ionosphere and produce polar cap auroras on the planet. That some loss must occur is evident from the pitch-angle distributions, whereas the particle beams are strongly unidirectional, with only a small component seen in the backscattered direction for both ions and electrons.

REFERENCES AND NOTES

1. L. J. Lanzerotti *et al.*, *Astron. Astrophys. Suppl. Ser.* **92**, 349 (1992).
2. Extensive summaries of the studies of the Jovian magnetosphere made by the Pioneer and Voyager spacecraft are included in special issues of the *Journal of Geophysical Research* [**79** (1 September 1974); **86** (30 September 1981)] and in *Physics of the Jovian Magnetosphere*, A. J. Dessler, Ed. (Cambridge Univ. Press, Cambridge, 1983).
3. The HI-SCALE instrument consists of five separate detector apertures in two separate telescope assemblies that are mounted by means of individual stub arms on a box containing the electronics. The instrument is mounted on one corner of the Ulysses spacecraft in order to provide unimpeded fields-of-view to the telescopes. Four of the detector apertures consist of back-to-back magnetic and foil spectrometers to separate electrons and ions. The composition aperture (CA) telescope provides a multiparameter separation of individual nuclear species. The energy passbands and orientations of the magnetic-foil spectrometers are such that a nearly complete 4π coverage of the solid angle is possible over a wide range of electron and ion energies. Unfortunately, some design compromises in the early stages of the instrument development, mandated during project definition, prevented some regions of angle–energy phase space from being covered.
4. S. M. Krimigis *et al.*, *J. Geophys. Res.* **86**, 8227 (1981).
5. R. D. Zwickl *et al.*, *ibid.*, p. 8125.
6. L. J. Lanzerotti *et al.*, in preparation.
7. The spacecraft locations during the Jupiter encounter are presented in an overview in this issue [E. J. Smith, K.-P. Wenzel, D. E. Page, *Science* **257**, 1503 (1992)].
8. L. J. Lanzerotti *et al.*, data not shown.
9. A. Balogh *et al.*, *Astron. Astrophys. Suppl. Ser.* **92**, 221 (1992).
10. The counting rates for the nuclei denoted as sodium or neon, magnesium, silicon (NMS) or both herein can include counts from other nuclei such as silicon and magnesium as well. However, because the abundances of these species in the Jovian magnetosphere are expected to be very low, we believe that essentially all of the rates we denote here as sodium are indeed sodium.
11. D. C. Hamilton *et al.*, *J. Geophys. Res.* **86**, 8301 (1981).
12. S. M. Krimigis *et al.*, *Science* **206**, 977 (1979).
13. A. L. Broadfoot *et al.*, *J. Geophys. Res.* **86**, 8259 (1981).
14. After the Pioneer and Voyager measurements of near-equatorial particles in the inner Jovian magnetosphere, there were extensive theoretical discussions of particle loss processes into the planet's atmosphere. See R. M. Thorne, in *Physics of the Jovian Magnetosphere*, A. J. Dessler, Ed. (Cambridge Univ. Press, Cambridge, 1983), pp. 454–488.

15. We express great thanks to our colleagues A. Balogh, Principal Investigator and R. Forsyth, Co-Investigator on the magnetometer team for sharing their data with us. We thank many people at our home institutions for their design, engineering, and software support over many years on behalf of this investigation, including R. Weitzmann, R. Campbell, R. Williams, D. Curtis, W. Frain, J. Dassoulas, B. Tossman, S. Gary, C. Tielens, D. Fort, A. Lew, S. Williams, D. Guynn, P. Schwartz, J. Mueller, C. Wingate, R. Thompson, B. Northrup, L. Staub, E. Hawkins, E. Keath, L. Suther, J. Townsend, K. Parker, G. Shelley, and L. Manweiler. The work on HI-SCALE at The Johns Hopkins University/Applied Physics Laboratory has been supported by NASA under Task I of contract N00039-89-C-0001 between The Johns Hopkins University and the Department of the Navy and by subcontract at the University of Kansas and the University of California.

1 June 1992; accepted 7 August 1992

Ulysses Radio and Plasma Wave Observations in the Jupiter Environment

R. G. Stone, B. M. Pedersen, C. C. Harvey, P. Canu, N. Cornilleau-Wehrlin, M. D. Desch, C. de Villedary, J. Fainberg, W. M. Farrell, K. Goetz, R. A. Hess, S. Hoang, M. L. Kaiser, P. J. Kellogg, A. Lecacheux, N. Lin, R. J. MacDowall, R. Manning, C. A. Meetre, N. Meyer-Vernet, M. Moncuquet, V. Osherovich, M. J. Reiner, A. Tekle, J. Thiessen, P. Zarka

The Unified Radio and Plasma Wave (URAP) experiment has produced new observations of the Jupiter environment, owing to the unique capabilities of the instrument and the traversal of high Jovian latitudes. Broad-band continuum radio emission from Jupiter and in situ plasma waves have proved valuable in delineating the magnetospheric boundaries. Simultaneous measurements of electric and magnetic wave fields have yielded new evidence of whistler-mode radiation within the magnetosphere. Observations of auroral-like hiss provided evidence of a Jovian cusp. The source direction and polarization capabilities of URAP have demonstrated that the outer region of the Io plasma torus supported at least five separate radio sources that reoccurred during successive rotations with a measurable corotation lag. Thermal noise measurements of the Io torus densities yielded values in the densest portion that are similar to models suggested on the basis of Voyager observations of 13 years ago. The URAP measurements also suggest complex beaming and polarization characteristics of Jovian radio components. In addition, a new class of kilometer-wavelength striated Jovian bursts has been observed.

The unique configuration, wide frequency range, and high sensitivity of the URAP instrument (*1*) have allowed many new observations to be made of both in situ and remote phenomena during the Ulysses-Jupiter encounter in early February 1992. The spacecraft's trajectory through high-latitude regions provided access to magnetospheric regions and radio source viewing geometries not available on previous missions (*2*). In addition, because of the retrograde nature of the trajectory, a large range of Jovian longitudes was surveyed during closest approach (CA), and the outbound trajectory was toward the Jovian dusk terminator.

The URAP sensors consist of a spin plane electric field dipole antenna (E_x), a spin axis electric field monopole antenna (E_z), and two magnetic search coils (B_y and B_z). The electric field measurements covered the frequency range from dc to 940 kHz, and the magnetic field measurements covered the frequency range from 0.08 to 448 Hz. The combination of magnetic and electric sensors made possible the first investigation of the electromagnetic nature of Jovian low-frequency emissions. The Ulysses radio astronomy receivers were specifically designed to measure simultaneously both the direction and the complete polarization state of a remote radio source. An active sounder provided additional in situ plasma measurements during the crossing of the Io torus.

R. G. Stone, M. D. Desch, J. Fainberg, W. M. Farrell, M. L. Kaiser, R. J. MacDowall, National Aeronautics and Space Administration Goddard Space Flight Center, Greenbelt, MD 20771.
B. M. Pederson, C. C. Harvey, S. Hoang, A. Lecacheux, R. Manning, N. Meyer-Vernet, M. Moncuquet, P. Zarka, Observatoire de Paris-Meudon, 92195 Meudon Principal Cedex, France.
P. Canu, N. Cornilleau-Wehrlin, C. de Villedary, Centre de Recherches en Physique de l'Environnement Terrestre et Planetaire (CRPE) CRPE/CNET/CNRS, 92131 Issy-les Moulineaux, France.
K. Goetz, P J. Kellogg, N. Lin, J. Thiessen, School of Physics and Astronomy, University of Minnesota, Minneapolis, MN 55455.
R. A. Hess, C. A. Meetre, V. Osherovich, M. J. Reiner, A. Tekle, Hughes STX, Lanham, MD 20706.

An overview of the radio data, covering the entire encounter period from just before the bow-shock crossing on 2 February 1992 (day 33) to just after the final outbound bow-shock crossing on 16 February 1992 (day 47), is illustrated in Fig. 1A. Times are indicated in spacecraft event time (SCET), which is universal time at the spacecraft. Above 40 kHz, a 10-hour periodicity produced by the planetary rotation is conspicuous. Below 25 kHz, very intense magnetospheric continuum radiation is observed throughout this period.

Magnetospheric boundaries. Characteristic radio and plasma wave emissions can be used to identify the region through which the spacecraft passed. For example, near Jupiter, the continuum radiation (*3*) is a ubiquitous phenomenon that is remarkably convenient for this purpose. The low-frequency cutoff of this broad-band emission indicates the in situ plasma frequency when the spacecraft is in the magnetosphere. Significant boundary crossings derived from the URAP data are listed in Table 1 and are discussed below.

Inbound. The URAP experiment first detected the escaping component of the Jovian continuum in late July 1991, when the spacecraft was about 1.6 astronomical units from Jupiter (*4*). These first observations showed that the portion of the continuum that exceeded the magnetopause cutoff fre-

Table 1. Major boundary crossings detected by URAP. The last column indicates the distance of the spacecraft from Jupiter in Jovian radii.

Event	Time		Distance
	Inbound		
Bow shock*	Day 33	17:33	113
Magnetopause		21:30 to 23:00	110 to 109
	Outbound		
Magnetopause out	Day 43	11:00 to 14:00	80 to 83
Magnetopause in		17:40	85
Magnetopause out		18:10 to 19:20	86 to 87
Bow shock out	Day 45	00:40	109
Bow shock in		04:30	112
Magnetopause in		16:05	120
Magnetopause out		20:45	124
Bow shock out	Day 47	07:50	149

*Identified by VHM/MAG.

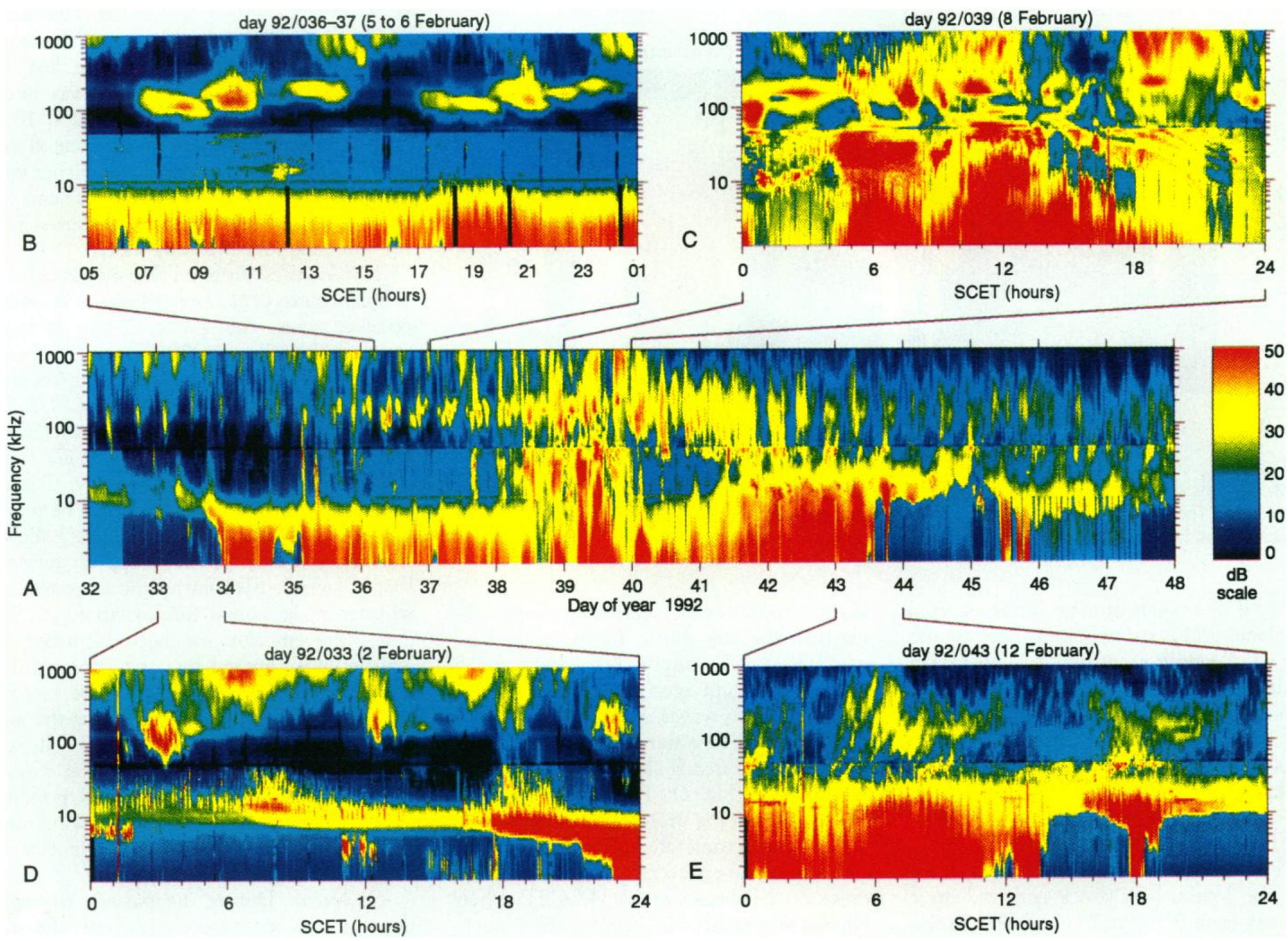

Fig. 1. URAP dynamic spectra during encounter displayed as frequency versus time, with relative intensity indicated by the color bar chart on the right. (**A**) Sixteen-day overview centered on CA (day 39). (**B**) Two typical Jovian rotations before CA, beginning at 05:00 SCET on 5 February (day 36). (**C**) Twenty-four–hour period centered on CA, including Io torus passage (day 39). (**D**) Twenty-four–hour period on the day of the inbound shock and magnetopause crossing. For this period only, the color bar covers the same color range but over the intensity scale of 0 to 35 dB (day 33). (**E**) Twenty-four–hour period containing some of the outbound magnetopause crossings (day 43).

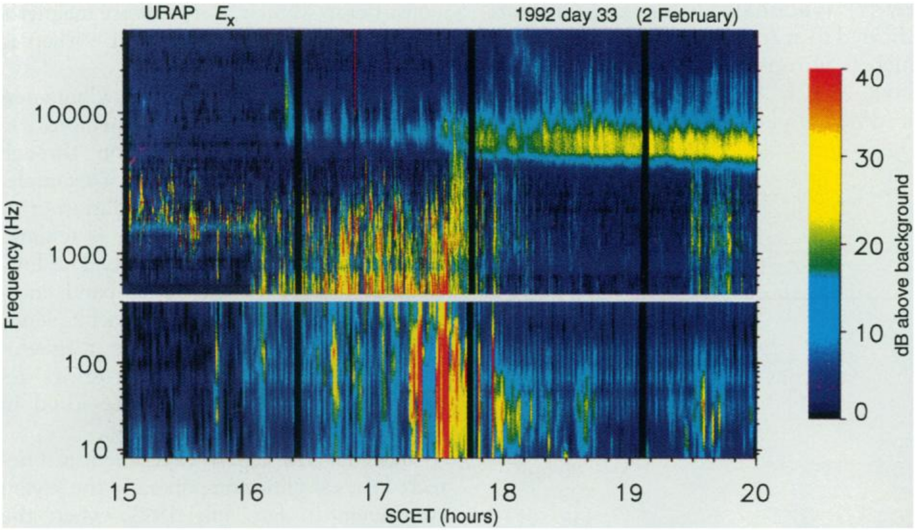

Fig. 2. Dynamic spectrum of the plasma and radio emissions observed close to the inbound bow-shock crossing, which occurred at 17:33 SCET. Impulsive bursts are evident before the shock crossing in the frequency range of 10 Hz to 3 kHz. The strongest emissions (shown in red) coincide with the shock crossing. The emission observed with a low-frequency cutoff at ~4 kHz is escaping continuum radiation. Examples of the fast-drifting "Jovian type III" bursts embedded in the continuum radiation are also evident.

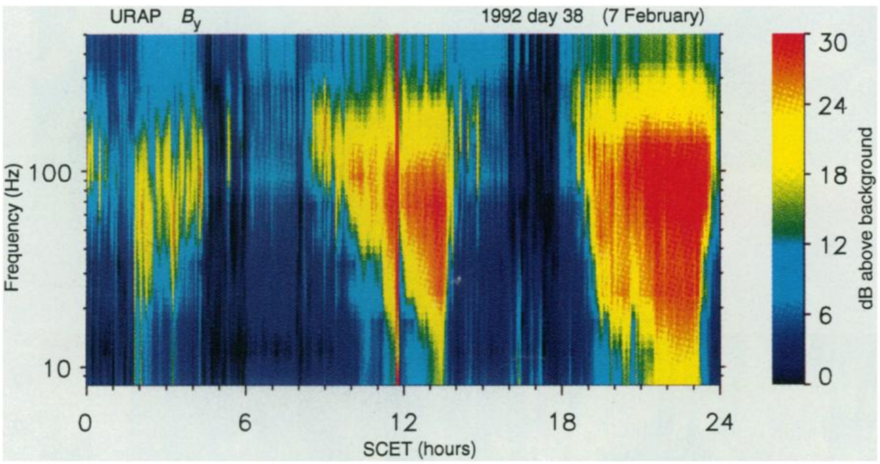

Fig. 3. Dynamic spectra of the B_y component of the magnetic search coil data in the frequency range 10 to 450 Hz. Three episodes of magnetic waves are seen around 02:00, 12:00, and 22:00 SCET, when Ulysses was at large magnetic latitudes. These electromagnetic waves are identified as auroral hiss.

quency is observable at great distances from the planet and is strongly influenced by the solar wind conditions at Jupiter. This Jovian continuum radiation is evident throughout 1 February (day 32) and most of 2 February (day 33) (Fig. 1, A and D), and the low-frequency cutoff gradually decreased from 9 to 6 kHz, indicating a decline of the electron density in the intervening Jovian magnetosheath from about 1.0 to 0.5 cm^{-3}.

Evidence of the imminent encounter with the Jovian bow shock occurred on 2 February from 00:00 to 01:50 SCET in the form of upstream electron plasma waves between 5 and 7 kHz (Fig. 1D). At this time Ulysses was at ~125 Jovian radii (R_J) (1 R_J = 71,398 km) from Jupiter. These waves (5) are excited near the solar wind plasma frequency by electrons back-streaming from the bow shock. Later, from 11:00 to 12:30 SCET, waves (between 3 and 5 kHz) were again seen. A third group of these upstream waves occurred from 14:30 to 17:30 SCET. After 16:00 SCET, they were accompanied by low-frequency waves below 1 kHz (Fig. 2). These may be caused by back-streaming protons.

The magnetometer experiment (6) indicated that the spacecraft crossed the bow shock on 2 February at 17:33 SCET, when Ulysses was about 113 R_J from the planet. At the same time, there was a significant enhancement in the continuum intensity in the URAP data (Fig. 1D), as well as a slight decrease in the low-frequency cutoff.

Electrostatic bursts in the frequency range between 10 Hz and 10 kHz were observed both upstream and downstream of the bow shock (Fig. 2). The largest amplitude was observed near the shock magnetic ramp (the current layer). Electromagnetic bursts were also detected downstream immediately after the shock and in the magnetosheath, possibly in the whistler mode.

At 21:30 SCET (110 R_J) there was an abrupt decrease in the continuum cutoff frequency (Fig. 1D) from 4 to 3 kHz, which coincided with the onset of extremely low-frequency (ELF) wave activity (10 to 100 Hz) and with an inbound magnetopause crossing identified by the magnetometer team (6). At 22:19 SCET a further sudden decrease to 2 kHz occurred, identified by the plasma experiment (7) as the magnetopause crossing. At about 23:00 SCET a dramatic change occurred in the continuum spectrum. The URAP experiment observed a trapped continuum spectrum for the first time: a spectral peak below 1 kHz with high-frequency radiation extending to ~20 kHz and—most important for identifying magnetospheric boundaries—a very low-frequency cutoff. This demonstrated that Ulysses had entered the magnetospheric cavity where, for the first 18 hours, the low-frequency cutoff was often below 300 Hz [electron density (N_e) < 10^{-3} cm^{-3})]. Thereafter, the continuum cutoff frequency quasi-periodically reached higher values, on the order of 2 kHz (N_e > 0.05 cm^{-3}), which is consistent with partial entries into the wobbling Jovian plasma sheet.

High latitudes. From 6 February through 11 February bursts of electromagnetic waves were observed when the spacecraft was at high magnetic latitudes (>20°). The electromagnetic nature of these emissions at Jupiter was confirmed unambiguously by the URAP search coil data. Both the electron cyclotron (6) and electron plasma frequency (7) were greater than the emission frequency. Consequently, the emission is believed to be propagating in the whistler mode. Figure 3 shows that the emission generally appears funnel-shaped, which is characteristic of terrestrial whistler-mode auroral hiss radiation (8, 9). Thus, the emission has been identified as whistler-mode auroral hiss at relatively high latitudes in the Jovian magnetosphere, usually above 30° magnetic latitude. During the auroral hiss events nearest CA, the Ulysses particle instrument (7) reported solar wind–like particle spectra at high latitudes, possibly resulting from the entry of the solar wind into an extended open magnetic field geometry in the Jovian magnetosphere.

Outbound. During the passage through the southern magnetosphere, both the intensity and the low-frequency cutoff of the continuum radiation were significantly modulated at the planet's apparent spin period; the minimum cutoff was associated with the maximum emission intensity and

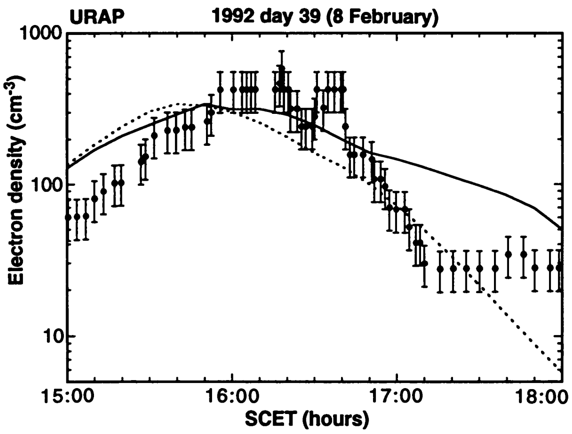

Fig. 4. Electron densities within the Io torus as determined from the plasma thermal noise spectra, with estimated uncertainties. For comparison, the dotted and continuous lines show the densities derived from the Divine and Garrett (*13*) and the new Bagenal Voyager models (*14*) calculated along the Ulysses trajectory.

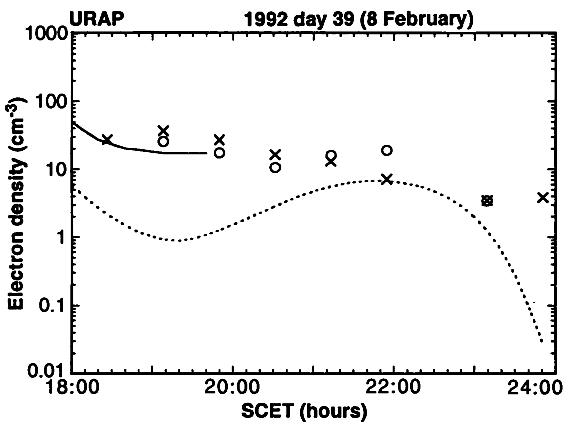

Fig. 5. Electron density near the Io torus as determined from the sounder. Points labeled "X" (average error ± 3%) and "O" (average error ± 30%) result from different interpretations of resonance lines (see text). The dotted curve is an extrapolation of the Divine and Garrett (*13*) model (derived from Voyager results) to the Ulysses trajectory, whereas the solid curve from the new Bagenal (*14*) model appears (over its limited range) to fit the data quite well.

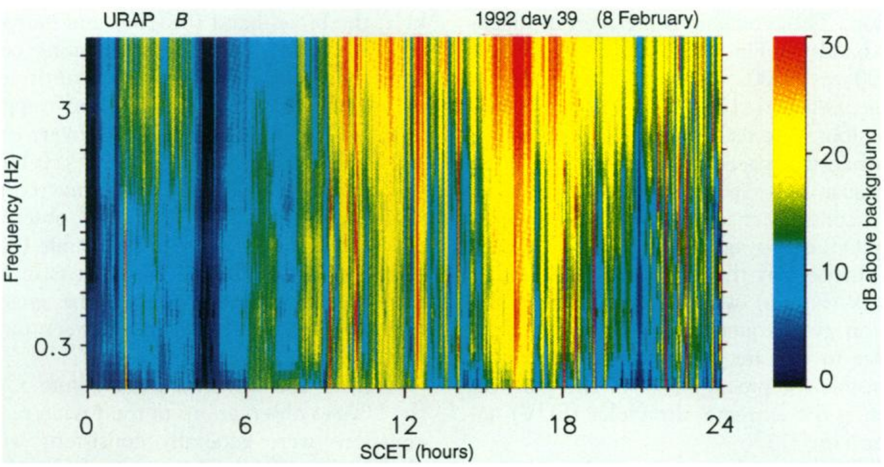

Fig. 6. Dynamic spectrum of one magnetic component (B_y or B_z) in the range 0.2 to 5 Hz for 8 February, the day of CA. Intense ULF waves are shown during the Io torus passage; relative intensity is indicated by the color bar chart on the right.

occurred at about 350° CML (System III central meridian longitude). The continuum was often observed to extend from a frequency of several hundred hertz to ~5 kHz. On 10 and 11 February (days 41 and 42) the continuum emission became very intense and extended up to ~25 kHz, suggesting that the magnetosphere had become compressed as a result of solar wind pressure enhancement (*4*).

The outbound encounter with the magnetopause and shock regions was more complex than the inbound leg, with multiple and partial boundary crossings, including a temporary excursion into the solar wind followed by a complete return to the magnetosphere. These outbound crossings identified from the URAP data are summarized in Table 1.

The spacecraft entered a magnetosheath-like boundary layer on 12 February at 10:55 SCET (Fig. 1, A and E), as indicated by a sudden increase in the continuum low-frequency cutoff from ~600 Hz to ~2 kHz. The changes in the cutoff suggest that at about 12:55 SCET the spacecraft was again within the magnetosphere, and from 13:30 to 13:57 SCET it reentered the sheath-like boundary layer. The first definitive outbound magnetopause crossing occurred at 13:57 SCET, as evidenced by the sudden sharp increase in cutoff of the continuum to ~7 kHz. Ulysses remained within the magnetosheath until about 16:45 SCET, when a boundary layer was encountered; this was followed by full magnetospheric reentry at 17:40 SCET, when intense continuum emission was detected down to 600 Hz. At 18:10 SCET Ulysses appeared to enter the sheath-like boundary layer once again, where it remained until the magnetopause was again crossed at 19:20 SCET.

Ulysses remained in the magnetosheath from 12 February at 19:20 SCET until it first encountered the bow shock on the outward leg on 14 February at 00:38 SCET (Fig. 1A, day 45). The wave spectrum at that time was typical of that seen upstream of quasi-perpendicular planetary bow shocks in the solar wind, a narrow band of Langmuir waves generated near the solar wind electron plasma frequency by electrons back-streaming from the shock. The upstream wave plasma frequency decreased suddenly at 01:50 SCET from about 11 to 6 kHz, as a result of the passage of an interplanetary shock. The consequent decrease in solar wind pressure allowed the Jovian magnetosphere to expand, sweeping the bow shock across the spacecraft at 04:30 SCET. Thereafter, the magnetosheath density decreased slowly and regularly until about 09:40 SCET, when the continuum cutoff frequency started to decrease more rapidly until 10:30 SCET. The spectrum suggests that either a magnetopause crossing occurred at about 10:30 SCET or the spacecraft started skimming along the edge of the boundary for several hours, at least until 14:30 SCET. From then until 16:05 SCET the continuum cutoff frequency was higher but fluctuated rapidly, perhaps indicating that Ulysses remained in the boundary layer. The spacecraft entered deeply into the magnetosphere at 16:05 SCET. Ulysses crossed the magnetopause abruptly at 20:45 SCET, remaining in the magnetosheath until the bow shock was crossed for the last time on 16 February (day 47) at 07:50 SCET.

In addition to these magnetospheric boundaries identified by the continuum observations, there is additional evidence of boundaries at ultra low frequency (ULF). Electromagnetic activity below 10 Hz was detected near the two magnetopause crossings of 12 February discussed above. Bursts of electromagnetic radiation below 20 Hz have been seen in association with the two shock crossings that occurred on 14 February. For all three shock crossings on the outbound leg, downstream whistler-mode waves were observed at ~10 Hz, and elsewhere in the magnetosheath bursts of electromagnetic waves were seen in the same frequency range.

Io torus densities. The electron density along the Ulysses trajectory within the Io torus was determined by two different techniques, utilizing either the quasi-thermal noise spectrum of the ambient plasma or the plasma resonances produced by the relaxation sounder. The instantaneous thermal noise spectrum, that is, the voltage induced by the random motion of the local electrons, permits determination of the in situ electron density and temperature when the electron gyrofrequency is much smaller than the electron plasma frequency (*10*). The plasma resonances stimulated by the relaxation sounder can be interpreted to determine ambient values for the electron density and the magnetic field strength on the basis of experience gained with sounders in Earth's orbit (*11, 12*).

During the passage through the densest part of the Io torus on 8 February (day 39) from 15:00 to 18:00 SCET, the quasi-thermal noise is the yellow band between 50 and 200 kHz (Fig. 1C). The electron density is deduced from the spectral shape of this band, whose low-frequency cutoff is near the upper hybrid frequency (which is very close to the plasma frequency during this interval). Figure 4 shows the density along the Ulysses trajectory obtained by this method together with densities derived from models on the basis of measurements made in 1979 on Voyager 1 (*13, 14*). The differences between the data and models are small in this region. The core electron temperature has been determined from the thermal noise spectra near 16:20 SCET. A value of $\sim 10^5$ K was found, which is also consistent with Voyager results.

The electron density near the outer region of the Io torus, as provided by the relaxation sounder, decreased from ~25 to $\sim 3\ \mathrm{cm}^{-3}$, as shown in Fig. 5. The density was determined with the use of two different techniques for interpreting the spectral features (resonances) stimulated by the sounder. In one technique (*11*), the resonances were interpreted as occurring at the gyroharmonics, the plasma frequency, the upper-hybrid frequency, and the Bernstein-mode Q resonances. In the other method (*12*), they were identified as being primarily attributable to the sequence of D resonances in addition to the plasma resonance and

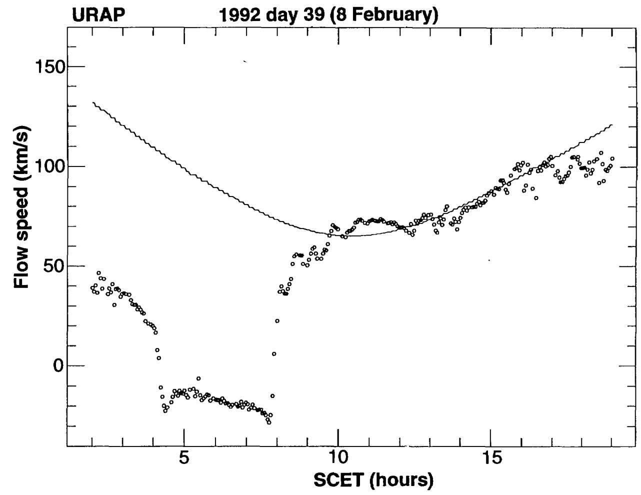

Fig. 7. Apparent flow speed (component in the corotation direction) covering CA and traversal of the Io torus. The solid line shows the corotation speed.

Q resonances. Both interpretations of the sounder data lead to densities significantly larger than those predicted by the Divine and Garrett model (*13*) on the outbound trajectory between 18:00 and 24:00 SCET; on the other hand, they are quite consistent with the applicable portion of the new Bagenal model (*14*).

Io torus plasma waves. The Ulysses spacecraft encountered a broad range of magnetic and plasma conditions throughout 8 February. Diffuse emissions between harmonics of the gyrofrequency (f_c) were observed in the low-frequency range of the radio receiver as Ulysses exited the torus region. These emissions are seen as diagonal bands in Fig. 1C from approximately 17:00 to 22:00 SCET, in the frequency range between 10 and 50 kHz. Intense emissions were recorded near $3/2\, f_c$ and $5/2\, f_c$, when the spacecraft crossed the magnetic equator (~16:15 SCET), confirming their confinement to this plane as observed by previous Voyager spacecraft (*15*).

Throughout the Io torus, intense ULF waves (Fig. 6) were observed below the proton gyrofrequency (f_{H^+}). Ion cyclotron waves in this frequency range may be responsible for precipitation of the particles causing the extreme ultraviolet (EUV) aurorae (*16, 17*).

Whistler-mode waves were also observed in the Io torus, at frequencies close to and above f_{H^+}. The strong signals observed up to 2 kHz (from 09:00 to 18:00 SCET) may be due to hiss, and those at about 10 kHz (from 10:30 to 13:00 SCET) may be due to chorus (*3*).

Plasma flow in the Io torus. Figure 7 shows the apparent flow speed on 8 February (deduced from the URAP dc potential difference of the E_x antennas, assuming an effective length of 36 m and that the flow is parallel to the corotation direction). Although there is close agreement between this speed and the corotation speed (solid line) in the interval from 09:30 to 17:30 SCET, the differences are significant. Outside this interval, the differences are attributed to insufficient antenna-plasma coupling. The low apparent flow speeds between 04:45 and 07:50 SCET are likely the result of entry into a region of low plasma density, the cusp, or polar cap. Data from the cosmic ray experiment (*18*) are consistent with this interpretation.

Jupiter as a radio source. The URAP frequency range covers most of Jupiter's well-known radio components (*19*): the hectometer (HOM) emission above ~300 kHz, the broad-band (bKOM) and narrowband (nKOM) kilometric emissions centered near 100 kHz, and the continuum emission in both its escaping and trapped form below about 25 kHz. Moreover, low-frequency fast-drift bursts near 10 kHz have been observed regularly. These may correspond to "Jovian type III bursts" observed previously by the Voyager spacecraft (*20*). The greater visibility of these bursts in the Ulysses data probably reflects the greatly increased sensitivity of the Ulysses radio receivers.

During the inbound pass, before CA, the Ulysses observations of the Jovian radio emissions were generally consistent with observations of previous spacecraft. Emphasized here are those radio observations near CA that are unique to the URAP instrument and to the high magnetic latitude of the Ulysses trajectory.

Source directions and polarizations. The observations of nKOM have demonstrated the unique capability of the URAP instrument for determining both source locations and polarizations. This radio emission is found to originate from a number of discrete sources at different locations in the outer regions of the Io plasma torus. These sources were tracked around Jupiter for many Jovian rotations, which allows a determination of their corotational lag, their spatial and temporal evolution, and their polarization characteristics. These observations are crucial for assessing the validity of models for nKOM radio emission (*21, 22*) and dynamical models of the Io plasma torus (*23*).

The nKOM emission (*24, 25*) is distinguished by its relatively narrow bandwidth and slow time variability compared with other Jovian radio emissions. Two periods of nKOM activity during two (~10-hour) consecutive Jovian rotations are shown in the dynamic spectrum in Fig. 1B. Each period of activity appears as several events lasting approximately 2 hours and centered at ~150 kHz. These two periods correspond to the same group of source regions located between about 60° and 330° CML observed during the two Jovian rotations.

The nKOM directions and polarization, at 148 kHz, determined from the URAP experiment are shown in Fig. 8 for the 10-hour interval corresponding to the first Jovian rotation in Fig. 1B. Figure 8A shows the observed flux as a function of SCET. The intensity variations with time suggest several individual nKOM sources; this is more clearly revealed in Fig. 8, B and C, which show the source azimuth and elevation, respectively.

The striking feature of the nKOM azimuth is the observed linear drift across the Ulysses-Jupiter line from dawn to dusk (east to west), as shown in Fig. 8B. This azimuthal drift reoccurred five times during the observed nKOM activity. At the same time, the source elevation was steady and mainly south of the Ulysses-Jupiter line (Fig. 8C). This behavior of the observed source azimuths and elevations is interpreted as corresponding to five individual source regions separated in Jovian longitude in corotational motion around Jupiter. The azimuthal excursion of about 10° for each source corresponds approximately to the angular width of the Io orbit (at ~6 R_J) viewed from Ulysses on day 36 [see (*2*) and Fig. 4, A and B, for the relevant spacecraft location relative to Jupiter]. The measured azimuthal drift rates imply that these source regions, in fact, lie at Jovicentric distances from about 8 to 10 R_J, that is, in the outer regions of the Io plasma torus. The radio emission from each of the individual sources was observed for a time interval corresponding to a partial Jovian rotation, suggesting that each nKOM source region had a finite beamwidth ranging from about 30° to 60°.

Similar results for the source azimuths and latitudes were observed for other frequencies within the nKOM emission and during other Jovian rotations, such as the second rotation in Fig. 1B. By comparing the observed azimuths of an individual nKOM source for two such consecutive Jovian rotations, one can precisely determine the corotational lag. Corotational lags ranging from 3 to 8% were determined for the individual nKOM sources in Fig. 8. The recurrence of the individual nKOM events over several Jovian rotations suggests distinct long-lived sources in the torus.

No significant linear polarization component was evident during this period of nKOM activity. The observed polarization shown in Fig. 8D was predominantly left-hand circular (LHC), and there was no obvious correlation with the individual nKOM source regions, as identified in Fig. 8B. There is, however, a striking correlation between LHC polarization and southern source latitudes, as in Fig. 8C. These properties of the polarization and latitude were observed consistently during the inbound pass. Left-hand circular polarization was dominant and was observed between about 120° and 320° CML, corresponding to the spacecraft at northern magnetic latitudes. This Jovian longitude region also corresponds approximately to the "active sector" of Jupiter's magnetosphere and Io torus (*26*).

High latitude observations. The observed morphology of HOM and bKOM is known to depend very sensitively on the observer's magnetic latitude, presumably because of narrow beaming of the radio emission (*27*). In contrast to previous spacecraft-Jupiter encounters, the very wide magnetic latitude excursions covered during the Ulysses-Jupiter encounter provide a unique opportunity for studying the variation of the radio emission with magnetic latitude, thereby establishing more precisely the beaming characteristics.

Owing to the 9.6° tilt of the Jovian magnetic axis relative to the rotational axis, the maximum magnetic latitude excursions of the Voyager spacecraft were 17°N and 6°S. In contrast, Ulysses reached maximum northern magnetic latitude of 48° at 06:30 SCET on 8 February. After CA, the southern magnetic latitude of Ulysses rapidly increased to about 46°S. From such high northern and southern magnetic latitudes, extensive changes were expected in the HOM, bKOM, and nKOM morphologies.

The dramatic change in character of the Jovian HOM radio emission observed during the inbound and outbound passes is evident from the central panel in Fig. 1. During the inbound pass, the 10-hour periodicity of the HOM emission is quite conspicuous. The most intense emission was consistently centered near 0° magnetic latitude, for example, at 06:30, 09:45, and 16:30 SCET on 2 February (Fig. 1D), even though the longitudes of the magnetic equator crossings were changing significantly from 1 to 6 February. These observations support narrow latitudinal beaming of the HOM emission along the magnetic equator, with no significant longitudinal dependence (*27, 28*). Intense HOM emission

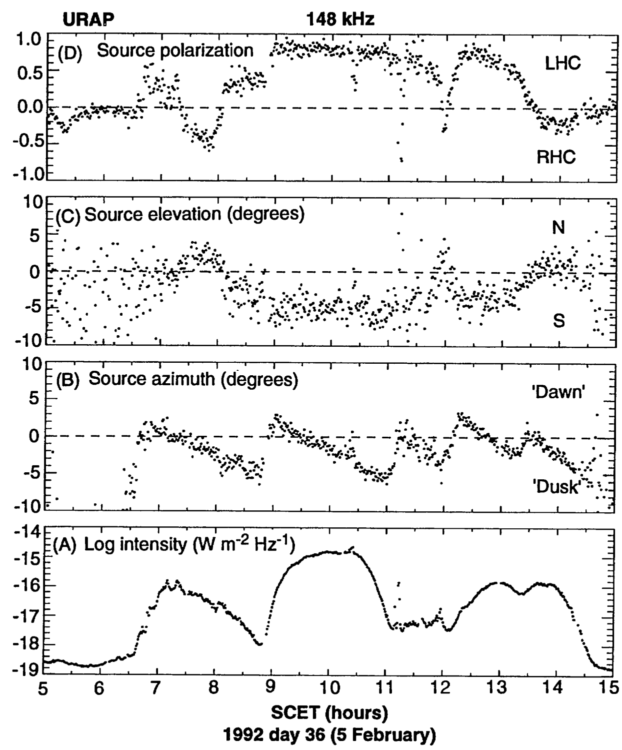

Fig. 8. (**A**) The nKOM source intensity at 148 kHz on 5 February 1992 as a function of SCET. (**B**) Derived source azimuth as viewed from Ulysses. Note the dawn to dusk drift in the source azimuth corresponding to each intensity maximum in (A). (**C**) Derived source elevation as viewed from Ulysses. During most of the nKOM activity, the source elevation lies to the south of the Ulysses-Jupiter line. The angles given in (B) and (C) are expressed in a coordinate system, fixed to the projection of Jupiter against the plane of the sky as viewed from the spacecraft; north points toward the ecliptic pole. In this system, the azimuth and elevation of Jupiter are always at 0°. (**D**) Degree of circular polarization: 100% LHC polarization corresponds to +1.0, 100% RHC polarization corresponds to −1.0. Note the correlation between the predominant LHC source polarization and the southern source elevations. Uncertainties are on the order of the scatter in the data points.

near the magnetic equator was observed as late as 01:30 SCET on 8 February, when the minimum magnetic latitude of Ulysses was 20°N, suggesting that the HOM beamwidth may be significantly larger than 20°. The HOM polarization was found to be complex, reversing between right-hand circular (RHC) and LHC. During the Io torus crossing, HOM emission was not observed, consistent with a shadow zone produced by the presence of the Io plasma torus (*29, 30*). During the outbound pass, when Ulysses passed through high southern latitudes, no emission appeared in the frequency range in which HOM was previously observed (Fig. 1E). The observed radio characteristics of the HOM emission outside the main equatorial beam (*31*) are complex and require further analysis.

As the spacecraft approached Jupiter, the bKOM (*32, 33*) morphology also changed dramatically. In Fig. 1D, intense, well-defined bKOM emission was observed centered at about 03:00 SCET (200° CML) between 40 and 200 kHz, when Ulysses was at a magnetic latitude of about 14°. The intense low-frequency striations extending to very low frequencies observed in the earlier bKOM activity (*34*) were now greatly reduced. Three days later, on 5 February (Fig. 1B), when Ulysses was at 17°, the bKOM emission (superposed on the much more intense nKOM emission) was barely visible at about 10:00 SCET (near 200° CML) at frequencies above 200 kHz. The entire low-frequency part of the bKOM spectrum, from 10 to 200 kHz, was absent. By the time of CA, bKOM became very fragmented.

Figure 1E shows typical URAP outbound observations covering two Jovian rotations. In the frequency range normally occupied by bKOM (20 to 200 kHz), an intense emission component consisting of many complex features and occurring essentially at all Jovian longitudes (with a slight diminution at ~200° CML, for example, 05:00 SCET on 12 February) is observed. These structures are reminiscent of the "arc" structure previously observed by Voyager in the range of 2 to 20 MHz. It is not clear if this emission is bKOM emission.

The above results illustrate the dramatic effects of magnetic latitude on the Jovian radio emissions, suggesting narrow latitudinal beaming of the radiation. The wide magnetic latitude excursions of Ulysses during CA provided, for the first time, crucial observations on the latitudinal extent and the radiation characteristics of the various radio emission beams.

Fast-drifting phenomena. Almost a year before encounter, URAP began observing low-frequency fast-drift bursts fairly regularly, and by the time of CA the bursts had become very common. These fast-drift phenomena are illustrated in the radio data on 2 February shown in Figs. 1D and 2. They extend in frequency from about 10 to 50 kHz and occur during most of the day, both before and after the bow-shock crossing at 17:33 SCET. Significant enhancements in the activity centered near 08:00 and 18:00 SCET (that is, near 20° CML) are evident, suggesting that the activity is modulated by the Jovian rotation. These bursts often appear to be quasi-periodic, and a period of 10 to 15 min separates individual bursts. This periodicity is particularly evident for the fast-drift bursts observed from 00:00 to 04:00 SCET in Fig. 1D, corresponding to 80° to 230° CML and magnetic latitude 0° to 14°N.

The morphology of these bursts changed or a new fast "drifting" phenomenon occurred during the southbound pass. Figure 1E shows fast periodic events extending from the low-frequency continuum to several hundred kilohertz. At a sweep-time resolution of 128 s, no measurable drift was detected. Although 40- to 45-min periodicity is evident in the most intense bursts, other shorter periodicities were also often seen. There is some indication that this activity is modulated with a 10-hour period. The origin of these phenomena is not understood; however, there appears to be some correlation of the outbound bursts with relativistic electron bursts (*18*).

Voyager Ulysses comparisons. One of the goals of the URAP Jupiter observations was to make a comparison with the Voyager observations made more than a decade ago. At the highest URAP frequencies, the hectometer wavelength source beaming pattern was measured, confirming the overlapping of northern and southern beams in the magnetic equatorial region deduced from Voyager observations. The bKOM emission revealed considerable fine structure at frequencies below 50 kHz that appeared in the form of striations in the frequency-time dynamic spectra. The exact form of these striations appears to be a function of the spacecraft position, and nearly "vertical" striations observed inbound are replaced with clear low-to-high frequency drifting striations outbound. The other kilometer component, nKOM, has been attributed to the outer torus region, near the magnetic equator (*24, 25*). With URAP, direct confirmation of this inference was obtained. Further, it was observed that the torus contains multiple radio sources, each emitting nKOM independently and rotating around Jupiter at slightly different rates.

With Voyager, a small number of fast-drifting quasi-periodic ("Jovian type III") events were detected within the Jovian magnetosphere. With the use of the superior URAP sensitivity, these fast-drifting events were found to be extremely common, and they must be considered to be a main component of Jupiter's radio spectrum. A study of possible correlations between the fast-drift bursts and periodic high-energy particle beams is in progress.

At the lowest radio frequencies, the Jovian continuum emission has been shown by URAP to be powerful enough to be observed throughout the outer solar system. Both the intensity and frequency range of the continuum have been observed to be a strong function of the solar wind ram pressure, thus providing a unique long-term remote monitor of solar wind conditions at Jupiter.

At plasma wave frequencies, the lowest continuum frequencies are trapped within the magnetosphere, unable to propagate through the high-density region of Jupiter's magnetosheath. The low-frequency cutoff of the trapped continuum provides a very visible marker of magnetospheric boundaries, as evidenced in Fig. 1A. The Io torus region was rich in plasma wave phenomena, quite reminiscent of the Voyager torus passages. The highest electron densities observed in the torus are remarkably similar to those observed by Voyager 1 13 years previously. The frequency resolution of URAP and the presence of the sounder, however, will enable a more complete understanding of the torus.

REFERENCES AND NOTES

1. R. G. Stone *et al.*, *Astron. Astrophys. Suppl. Ser.* **92**, 291 (1992).
2. E. J. Smith, K.-P. Wenzel, D. E. Page, *Science* **257**, 1503 (1992).
3. D. A. Gurnett and F. L. Scarf, in *Physics of the Jovian Magnetosphere*, A. J. Dessler, Ed. (Cambridge Univ. Press, New York, 1983), p. 285.
4. M. L. Kaiser *et al.*, *Geophys. Res. Lett.* **19**, 649 (1992).
5. P. C. Filbert and P. J. Kellogg, *J Geophys. Res.* **84**, 1369 (1979).
6. A. Balogh *et al.*, *Science* **257**, 1515 (1992).
7. S. J. Bame *et al.*, *ibid.*, p. 1539.
8. D. A. Gurnett and L. A. Frank, *J. Geophys. Res.* **83**, 1447 (1978).
9. D. A. Gurnett, in *High Latitude Space Physics*, B. Hultquist and T. Hagfors, Eds. (Plenum, New York, 1983), pp. 355–375.
10. N. Meyer-Vernet and C. Perche, *J. Geophys. Res.* **94**, 2405 (1989).
11. J. Etcheto and J. J. Bloch, *Space Sci. Rev.* **22**, 597 (1978).
12. V. Osherovich and R. F. Benson, *J. Geophys. Res.* **96**, 19331 (1991).
13. N. Divine and H. B. Garrett, *ibid.* **88**, 6889 (1983).
14. F. Bagenal, personal communication.
15. W. S Kurth, D. D. Barbosa, D. A. Gurnett, F. L. Scarf, *Geophys. Res. Lett.* **7**, 57 (1980)
16. D. A. Gurnett and C. K. Goertz, *ibid.* **10**, 587 (1983).
17. R. M. Thorne and J. Moses, *ibid.*, p. 631.
18. J. A. Simpson *et al.*, *Science* **257**, 1543 (1992).
19. T D Carr, M. D. Desch, J. K. Alexander, in *Physics of the Jovian Magnetosphere*, A. J. Dessler, Ed. (Cambridge Univ. Press, New York, 1983), p. 226.
20. W. S. Kurth, D. A. Gurnett, F. L. Scarf, *J. Geophys. Res* **94**, 6917 (1989).
21. D. Jones, *Nature* **327**, 492 (1987).
22. S. F. Fung and K. Papadopoulos, *J. Geophys. Res.* **92**, 8579 (1987).
23. Y. S. Yang *et al.*, *Geophys. Res. Lett.* **19**, 957 (1992)

24. M. L. Kaiser and M. D. Desch, *ibid.* 7, 389 (1980).
25. G. Daigne and Y. Leblanc, *J. Geophys. Res.* **91**, 7961 (1986).
26. T. W. Hill, A. J. Dessler, C. K. Goertz, in *Physics of the Jovian Magnetosphere*, A. J. Dessler, Ed. (Cambridge Univ. Press, New York, 1983), p. 353.
27. J. K. Alexander, M. D. Desch, M. L. Kaiser, J. R. Thieman, *J. Geophys. Res.* **84**, 5167 (1979).
28. H. P. Ladreiter and Y. Leblanc, *Ann. Geophys.* **8**, 477 (1990).
29. J. L. Green and D A. Gurnett, *Geophys Res. Lett.* **7**, 65 (1980).
30. H. P. Ladreiter and Y. Leblanc, *J. Geophys. Res.* **95**, 6423 (1990).
31. ______, *ibid.* **96**, 21207 (1991).
32. M. D. Desch and M. L. Kaiser, *ibid.* **85**, 4248 (1980).
33. Y. Leblanc and G. Daigne, *ibid.* **90**, 12073 (1985).
34. A. Lecacheux *et al.*, *Geophys. Res. Lett.* **19**, 1307 (1992).
35. We thank R. F. Benson for review of this paper and helpful suggestions and A. Meyer and A. Morane for help with data analysis. The French contribution was financed by the Centre National d'Etudes Spatiales. The French laboratories are associated with the CNRS and are partially funded by this organization via the Institut National des Sciences de l'Univers.

1 June 1992; accepted 31 July 1992

Ulysses Radio Occultation Observations of the Io Plasma Torus During the Jupiter Encounter

M. K. Bird, S. W. Asmar, J. P. Brenkle, P. Edenhofer, O. Funke, M. Pätzold, H. Volland

Radio signals from Ulysses were used to probe the Io plasma torus (IPT) shortly after the spacecraft's closest approach to Jupiter. The frequencies of the two downlinks at S-band (2.3 gigahertz) and X-band (8.4 gigahertz) were recorded, differenced, and integrated in order to derive the columnar electron density of the IPT. The measurements agree qualitatively with contemporary models of the IPT based on Voyager data, but significant differences are apparent as well. The overall level of the IPT electron density is approximately the same as the prediction, implying that the amount of gas (or plasma) injected from Io is similar to that observed during the Voyager era. On the other hand, the IPT seems to be less extended out of the centrifugal equator, implying a smaller plasma temperature than predicted.

The Ulysses spacecraft was occulted by the IPT during its Jupiter encounter on 8 February 1992. The Ulysses dual-frequency radio subsystem used by the Ulysses Solar Corona Experiment (SCE), which was primarily intended for coronal radio sounding investigations and was used during the solar conjunction from July to September 1991 (*1*), was utilized to measure the electron content (column density) of the IPT. The IPT during the Ulysses flyby at Jupiter was found to be slightly higher in peak electron density but slightly lower in mean electron content than predicted by the Voyager-based models. The unique Ulysses occultation geometry was favorable for discriminating between contributions from the sections of the IPT in front of and behind Jupiter, respectively. Initial analysis of the electron content profile indicates that these two contributions are quite different, implying longitudinal asymmetry of the IPT.

The first two spacecraft to fly behind the IPT, Pioneer 10 and Pioneer 11, transmitted only a single S-band downlink. The Doppler shifts of this radio signal caused by the occultation of the IPT are now known to be $\approx$10 mHz, a value too small to be easily distinguished from other nondispersive perturbations in frequency. Dual-frequency occultations of the IPT occurred during the Jupiter flybys of Voyager 1 and Voyager 2 (5 March and 9 July 1979, respectively). A clear signature of the IPT was obtained at the Voyager 1 flyby (*2*). After corrections for the terrestrial ionosphere had been removed, a peak electron content of some 60 hexems (*3*) was attributed to the IPT (*4*). A more comprehensive analysis of the data (*5*), undertaken with the goal of deriving a more precise mass determination of the Galilean moons, revealed the IPT on the ingress and egress legs of both Voyager trajectories. The IPT electron content measured during the Voyager 2 flyby has not been analyzed in detail (*6*).

It is known that the IPT plane of symmetry is the "centrifugal equator," a plane lying between the rotational equator and the magnetic equator (*7–9*). For this work, it was assumed that the centrifugal equator was tilted by 6.5° with respect to the Jovian rotational equator. This is $2/3\alpha$, where $\alpha = 9.8° \pm 0.3°$ is the dipole tilt angle (*9*). Because the plasma is forced to corotate with the Jovian magnetic field, the IPT wobbles synchronously about Jupiter with the planet's rotation. In order to more effectively display the relation of the IPT to the Ulysses spacecraft and its radio ray path to Earth, Fig. 1 shows three orthogonal views of the Jupiter flyby geometry near the time of Jupiter closest approach (JCA) in a nonrotating "centrifugal" coordinate system. The IPT is stationary in this reference frame.

The z axis of Fig. 1 is perpendicular to the centrifugal equatorial plane. With $\hat{z}$ a unit vector along the z axis, the y axis is chosen perpendicular to the z axis and perpendicular to the Jupiter-Earth vector $\mathbf{r}_{JE}$, such that $\hat{y}$ is given by $\hat{z} \times \mathbf{r}_{JE}/r_{JE}$. The remaining x axis points such that the x, y, and z axes form an orthogonal triad with origin at Jupiter's center. The stylized IPT in Fig. 1 is roughly defined by the electron density contour of $N_e = 1000$ electrons per cubic centimeter. For simplicity, it is taken here to be a symmetric ring, centered on Jupiter, with maximum plasma density at a Jovian distance of 5.5 Jovian radii (R_J). The cross section of the IPT was taken to be elliptical; the radial thickness $d_\rho = 2\ R_J$ and the latitudinal thickness $d_z = 1\ R_J$. The ray paths to Earth are all parallel to the x–z plane, but they change slope in this coordinate system because of the above mentioned wobble (seen best in Fig. 1B). An isometric view of the IPT occultation in this coordinate system from a vantage point above the centrifugal equator may be found in the SCE instrument description (*1*).

The timing of the flyby was such that the ray path first penetrated the IPT in front of Jupiter and then the section closer to Ulysses in back of Jupiter. This situation was not fortuitous. Various mission restrictions were imposed on the Ulysses flyby trajectory at Jupiter in order to assure safe passage of the spacecraft and an optimum postencounter heliocentric trajectory. These restrictions precluded a radio occultation by Jupiter itself. It was also impossible to design a flyby through the IPT density maximum that would still comply with the safety requirement that the Ulysses perijove be greater than 6 R_J. An occultation of the spacecraft by the IPT, however, could "hardly be avoided." Another requirement stipulated that the energetic particle radiation fluence on the Ulysses spacecraft be a minimum. This was accomplished by minimizing the travel time through the IPT, that is, by choosing the encounter time such that the motion of the IPT was opposite to that of the spacecraft. Ulysses thus flew quickly through the Jovian centrifugal equator, just grazing the outer edge of the IPT. The total time spent in the IPT sector behind Jupiter, for both in situ and radio sounding measurements, was only

M. K. Bird, O. Funke, H. Volland, Radioastronomisches Institut, Universität Bonn, 5300 Bonn, Germany.
S. W. Asmar and J. P. Brenkle, Jet Propulsion Laboratory, California Institute of Technology, Pasadena, CA 91109.
P. Edenhofer, Institut für Hochfrequenztechnik, Universität Bochum, 4630 Bochum, Germany.
M. Patzold, Deutsche Forschungsanstalt für Luft- und Raumfahrt, 8031 Oberpfaffenhofen, Germany.